



Electrochemical Impedance of Hydrogenated Phases of ZnO and CuO Nanoparticles for Electrode Applications

L. I. Menegbo¹, J. L. Konne^{1*} and N. Boisa¹

¹Department of Chemistry, Rivers State University, Nkpolu-Oroworukwo, Port Harcourt, Nigeria.

Authors' contributions

This work was carried out in collaboration among all authors. Author LIM designed the study, performed the statistical analysis, wrote the protocol and wrote the first draft of the manuscript. Authors JLK and NB managed the analyses of the study. Author JLK managed the literature searches. All authors read and approved the final manuscript.

Article Information

DOI: 10.9734/AJOPACS/2020/v8i330116

Editor(s):

(1) Dr. Thomas F. George, University of Missouri-St. Louis, USA.

Reviewers:

(1) Mohammad Musarraf Hussain, Jagannath University, Bangladesh.

(2) P. Geetha, GMRIT, India.

(3) Mohd Husairi bin Fadzilah Suhaimi, Universiti Teknologi MARA, Malaysia.

Complete Peer review History: <http://www.sdiarticle4.com/review-history/58027>

Short Communication

Received 06 April 2020

Accepted 13 June 2020

Published 22 June 2020

ABSTRACT

The Electrochemical Impedance Spectroscopy (EIS) measurements of Sol-gel synthesized ZnO, CuO and their respective hydrogenated phases (ZnO:H and CuO:H) for a proton-type battery model has been reported for the first time. The XRD patterns confirmed that CuO and ZnO were phase pure with minor impurities. However, that of CuO:H showed mixed phases of CuO and Cu₂O with the later appearing prominent. The estimated particle sizes of ZnO, ZnO:H, CuO and CuO:H obtained using Scherrers' equation were 17.83, 17.75, 21.63 and 15.42 nm respectively, showing remarkable particle size reductions upon hydrogenation as oxygen vacancies were substituted with smaller hydrogen ions. Nyquist plots from the EIS experimental data recorded over a frequency range of 100 kHz – 5 mHz showed expected flat semicircles at the high frequency region and straight lines at the low frequency regions while resistance estimations from the intercepts of the Bode plots were 12.10, 7.80, 16.00 and 10.80 Ω for ZnO, ZnO:H, CuO and CuO:H respectively. It also indicated high gain margins suggesting impressive electrochemical properties for battery applications.

*Corresponding author: E-mail: joskonne@gmail.com, konne.joshua@ust.edu.ng, konne.jsouha@ust.edu.ng;

Keywords: Defects; sol-gel preparation; battery; ZnO/ZnO:H; CuO/CuO:H; EIS (Nyquist &Bode).

1. INTRODUCTION

Transition metal oxide nanostructures have gained much research interest lately owing to their wide spectrum of properties harvestable by scientists and engineers for diverse applications. This characteristic non-stoichiometric nature is responsible for the inherent vacancies and defects in their crystal lattices. As a result, they function in catalysis, drug delivery and sensor building amongst others. Two of the most common and environmentally friendly 3-d transition binary metal oxides of interest are ZnO and CuO [1-3].

ZnO and CuO exist in two non-stoichiometric metal oxides (MO) Phases; $M_{1-x}O$ or MO_{1-x} which is often a function of which metal atom is electron deficient or rich. The metal deficient phase is a strong electron acceptor, while the oxygen deficient phase is a strong donor. In the donor form (MO_{1-x}), ZnO or CuO shows good n-type semiconductivity with an increase in electrical conductivity following the promotion of electrons to the conduction band. The presence of associated impurities such as hydrogen on the oxygen sites account for the oxygen deficient phase [1]. First principle calculations drawn from the estimation of the role of hydrogen loading on the electronic properties of ZnO showed that Interstitial hydrogen behaves like a shallow donor with only the positive charge state (H^+) being thermodynamically stable [4,5].

However, CuO has a narrower band gap than ZnO. It is a semiconductor with interesting characteristic properties similar to ZnO as both have been used as anode electrode material for lithium ion batteries (LIBs) and other applications. On the other hand, the hybrid CuO-ZnO pn junction has been used as photocatalyst for the photochemical splitting of water molecules to generate hydrogen solar fuel [6-8].

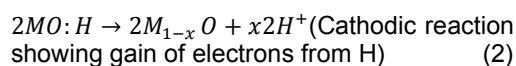
Recent reports on the successful sol-gel synthesis of ZnO/ZnO:H and CuO/CuO:H phases suggested possible application of these pairs as electrode materials for proton conduction [1,2]. A proton driven battery is viewed as an alternative to Lithium Ion Batteries (LIBs) as the World moves towards zero emission of green house gases. Lack of recyclability of used LIB electrodes is rapidly depleting Li metal reserves making LIB technology non-sustainable. Researchers have

shown that proton batteries demonstrated zero mass loss, better comparative cycle stability to LIBs, good energy efficiency and ultra low temperature stability. Electrode materials such as graphite composite with MnO_2 , MoO_3 , and activated carbon have been used in such systems [9,10]. Till date, there seems to be no report on the possible use of cheap and available transition metal oxides and their hydrogenated forms for proton battery systems. In addition, the EIS studies of these materials have also not been reported. This work seeks to investigate the syntheses, hydrogenation and EIS measurement of these pairs (ZnO/ZnO:H and CuO/CuO:H) in order to establish suitability for electrode applications in a novel proton-type conduction battery system.

2. EXPERIMENTAL

2.1 Syntheses of CuO and ZnO Nanoparticles and their Hydrogenated Phases

20 ml of 1.0 M $CuSO_4 \cdot 5H_2O$ was dissolved in 20 ml starch solution prepared by the dissolution of 3.0 g of starch in 15 ml 0.5 M acetic acid solution. The same protocol was used for $ZnSO_4 \cdot 7H_2O$ in place of the $CuSO_4 \cdot 5H_2O$ in a separate beaker. Subsequently, 10 ml of 0.5 M NaOH was added to form precipitates of copper hydroxide and zinc hydroxide, respectively. The precipitates were washed, filtered and oven dried for 12 h at 80°C to form dry flakes (hydroxide-starch composites). This was ashed in a muffle furnace for 4 h at 550°C to form copper (II) oxide (CuO) and Zinc (II) oxide (ZnO) respectively. The samples were characterized using X-ray diffractometer and Electrochemical Impedance Spectroscopy. The hydrogenated metal oxides (MO:H) were formed by passing H_2 gas generated from the reaction of magnesium ribbon in 20 ml aqueous hydrochloric acid (HCl) directly unto the synthesized metal oxides in a small test tube for 10 minutes as shown in Fig. 1. The half cell reaction mechanisms for the proposed rechargeable coin cell battery are illustrated in 1 & 2 where M represents Zn or Cu.



The liberated H^+ ion from the cathode migrates through a separator membrane containing protic electrolyte to the anode where it gains electron and become interstitial H atom in the lattice of the host (anode). The vacancies, defects and affinity of MO to hosting of small molecules could favour this reaction mechanism while the reverse reaction occurs during charging.

polytetrafluoroethylene (PTFE) in ethanol using a weight ratio of 8:1:1 to form a slurry. After solvent evaporation, the electrode was pressed and dried at $120^\circ C$ under vacuum for 24 h. The salt $LiPF_6$ was dissolved in a mixture of ethylene carbonate (EC), ethyl methyl carbonate (EMC) and dimethyl carbonate (DMC) (1:1:1, v/v) to form a 1.0 M electrolyte solution.

2.2 Electrochemical Impedance Spectroscopy

The Electrodes were prepared by mixing the sample powders with acetylene black and

The EIS studies were performed at ambient temperature with a potentiostat (Autolab PGSTAT 30 ECO CHIMIE) and an electrode cell containing 200 cm^3 of electrolyte. A saturated calomel electrode (SCE) and Li foil were used respectively as reference and auxiliary electrode.

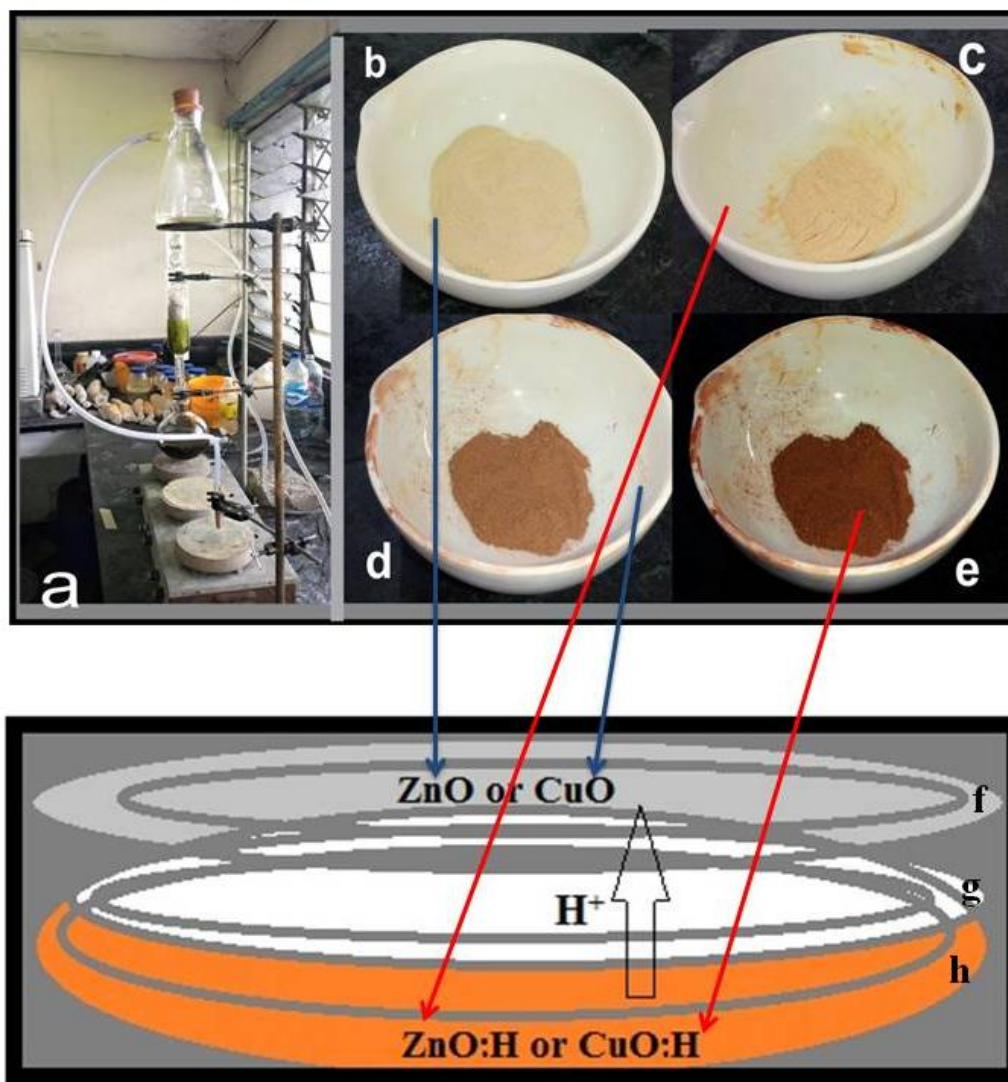


Fig. 1. (a) Hydrogenation set up (b) ZnO (c) ZnO:H (d) CuO (e) CuO:H and proposed coin cell with (f) ZnO or CuO anode (g) spacer/protic electrolyte and (h) ZnO:H or CuO:H cathode

The measurements were carried out in the 10 mV perturbation amplitude in the range from 100 kHz to 5 MHz in automatic sweep mode from high to low frequencies. A plot of the imaginary component of impedance (Z'') versus the real component of impedance (Z') called Nyquist plot and that of impedance against frequency with dual component of gain and phase (upper and lower) parts (Bode plot) were drawn. The phase portion shows the stability of the system while the intercept on the vertical axis of a Bode diagram provides direct reading of the resistance (R) which in turn has an inverse relationship with conductivity (σ) as derived from Pouillet's law (equation 3 and 4).

$$R = \rho \frac{l}{A} \quad (3)$$

Where

ρ , l and A are Resistivity, lenght of electrode and cross sectional area of electrode respectively.

$$\text{Conductivity } \sigma = \frac{1}{\rho} \quad (4)$$

3. RESULTS AND DISCUSSION

The X-ray diffraction patterns of the four samples are shown in Fig. 2. The particle sizes were estimated based on Scherrer's equation to be 17.83, 17.75, 21.63 and 15.42 for ZnO, ZnO:H, CuO and CuO:H respectively. The occupation of smaller hydrogen ions on the oxygen or transition metal ion sites could be responsible for the observed reduction in particle sizes of the ZnO:H and CuO:H and increased presence of impurity peaks [1,2]. The XRD pattern of ZnO with triplet peaks (at 2-theta = 31, 34 and 36 °) was indexed to a hexagonal zincite-type structure with the Joint Committee on Powder Diffraction Standards (JCPDS) card number 05-0664 [2]. Similar trend was also observed for CuO and CuO:H as shown in Fig. 2b. Sharp intense peaks at 35.4 ° and 39.2 ° positions were indexed to JCPDS card number 45-0937 [8,10] while CuO:H has only one intense peak that matched with the CuO phase at 35.53°. The other major peaks matched with Cu₂O pattern with JCPDS card number 05-0667 [11,12]. Hydrogenation could be responsible for the reduction of Cu²⁺ to

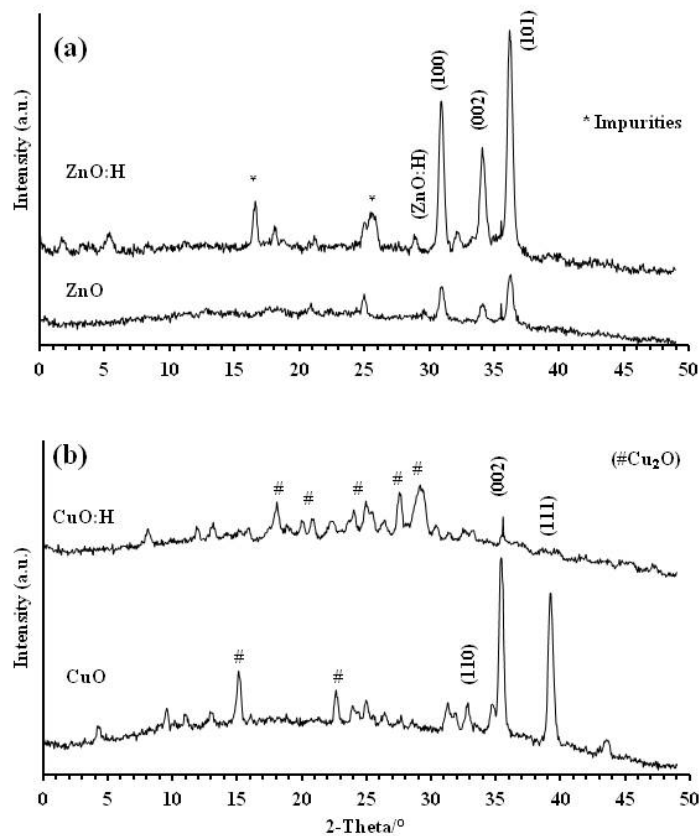


Fig. 2. XRD reflections of (a) ZnO/ZnO:H and (b) CuO/CuO:H

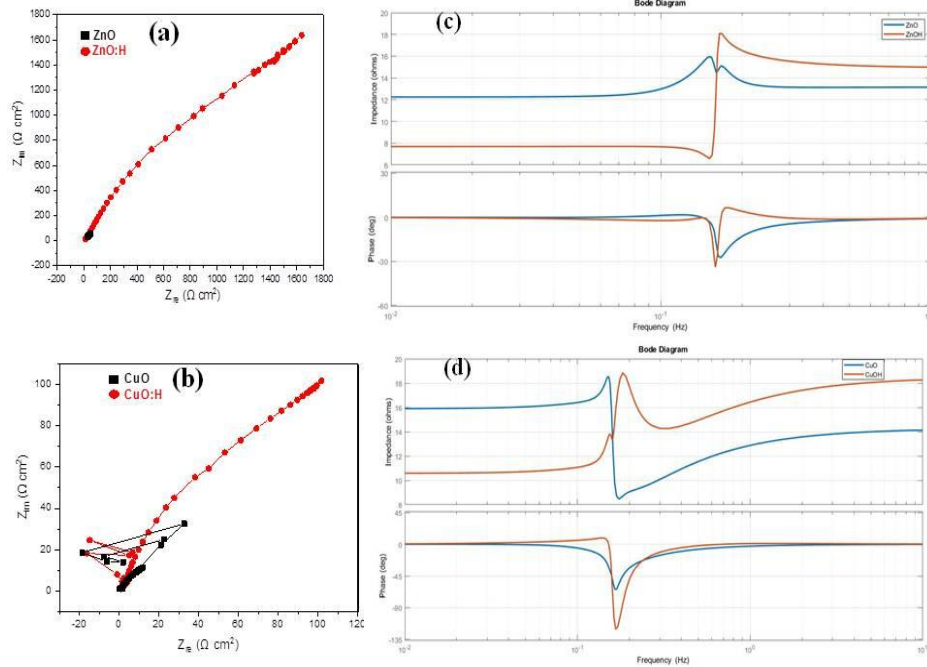


Fig. 3. Nyquist and Bode plots of (a, c) ZnO & ZnO:H and (b, d) CuO & CuO:H respectively

Cu^+ . Formation of brownish coloured Cu_2O as a result of disproportionation reaction of Cu and Cu^{2+} to form Cu_2O has been reported in literature [12]. This could be responsible for the larger observed difference in particle sizes of CuO and CuO:H compared to their zinc analogues where such reduction was not thermodynamically favoured. Starch-mediated ZnO:H has been associated with a peak at 2-theta 29.6° and similar small peak was observed at 2-theta 29° in Fig. 2a [1]. The impurities at 2-theta 16.6 and 25.5° might be due to ZnO minor hydrated phases but could not be indexed to any known phase with the available data.

The Nyquist combined plots of ZnO/ZnO:H and CuO/CuO:H electrodes under investigation displayed flat semicircles at the high frequency regions reflecting a high conductivity and charge transfer process corresponding to ionic diffusion through the solid electrolyte interface (SEI), while the near straight lines at the low frequency regions indicated diffusion processes linked with Warburg resistance (Fig. 3a and b). Few outliers probably due to some complex transport mechanisms involved in the charge transfer and diffusion processes occurring at the SEI were also observed in CuO. Reduction of the charge transfer Resistance (R_{ct}) obtained for ZnO:H and CuO:H phases led to higher charge transfer rates. Thus H atoms in the interstitial

positions / holes of ZnO and CuO lattices acted as electron mediators in the charge transfer processes [1,5].

These results showed that H acted as an exclusive positive charge state (donor) that promoted an improved conductivity contrary to experimentally and theoretically known amphoteric behavior which often counteract conductivity of materials [5]. The gain component of ZnO Bode plot showed a resistance of 12.1 Ohms while 7.8 Ohms was recorded for ZnO:H. Lower resistance values have been reported for nano ZnO compared to commercial ZnO. This implied that the lower resistance obtained here could be a combination of the effects of size and the enhanced conductivity due to added electrons from the H-atoms [13]. Similarly, CuO showed a resistance of 16 ohms and a much more reduced resistance of 10.8 Ohms for CuO:H (Fig. 3c and d).

4. CONCLUSION

Sol gel syntheses and characterization of ZnO, ZnO:H, CuO and CuO:H for electrode application has been investigated. The XRD patterns of the samples confirmed that the samples were phase pure with minor impurities except CuO:H that was indexed to mixed phases of CuO and Cu_2O . EIS Data and

its derivatives (Nyquist and Bode plots) respectively showed improvement in the conductivities and capacitive properties of the materials with hydrogenation which will provide the potential difference required to drive a battery system. Therefore ZnO/ZnO:H and CuO/CuO:H represent two sets of proton-type battery system for development as alternative rechargeable battery systems.

ACKNOWLEDGEMENTS

The authors wish to express appreciation to Technologist Chizam Oti of the Center for Petroleum Geoscience, University of Port Harcourt for the XRD analysis. We also like to thank Dr Nkem Iroha of Chemistry Department, Federal University Otuoke, Bayelsa State and Mr. Willy I. Briggs of Rivers State University, Port Harcourt for their assistance with the Nyquist and Bode plots.

COMPETING INTERESTS

Authors have declared that no competing interests exist.

REFERENCES

1. Konne JL, Christopher BO. Sol-Gel syntheses of zinc oxide and hydrogenated zinc oxide (ZnO:H) Phases. *Journal of Nanotechnology*. 2017;5219850:8.
2. Konne JL, Arinze AU. Hydrogenation of cashew kernel oil using green synthesized CuO and CuO:H as catalyst. *Journal of Chemical Society of Nigeria*. 2019;44:285-291.
3. Hussain MM, Asiri AM, Rahman MM. Simultaneous detection of L-aspartic acid and glycine using wet-chemically prepared Fe₃O₄@ZnO nanoparticles: Real sample analysis. *Royal Society of Chemistry Advances*. 2020;10:19276-19289.
4. Muth J, Kolbas R, Sharma A, Oktyabrsky S, Narayan J. Excitonic structure and absorption coefficient measurements of ZnO single crystal epitaxial films deposited by pulsed laser deposition, *Journal of Applied Physics*. 1999;85:7884-7887.
5. Zhang Z, Look D, Schifano R, Johansen K, Svensson B, Brillson L. Process dependence of H passivation and doping in H-implanted ZnO. *Journal of Physics D: Applied Physics*. 2013;46:055107.
6. Sathiya S, Okram G, Jothi M. Structural, optical and electrical properties of copper oxide nanoparticles prepared through microwave assistance. *Advance Materials Proceedings*. 2017;2:371-377.
7. Zhang W, Du L, Chen Z, Hong J, Yue L. ZnO nanocrystals as anode electrodes for lithium-ion batteries. *Journal of Nanomaterials*. 2016;8056302:7.
8. Lashgari M, Elyas-Haghighi P, Takeguchi M. A high efficient pn junction nanocomposite solar-energy-material [nanophotovoltaic] for direct conversion of water molecules to hydrogen solar fuel. *Solar Energy Materials & Solar Cells*. 2017;165:9-16.
9. Heidari S, Mohammadi SS, Oberoi AS, Andrews J. Technical feasibility of a proton battery with an activated carbon electrode. *International Journal of Hydrogen Energy*. 2018;153:1-13.
10. Yan L, Huang J, Guo Z, Dong X, Wang Z, Wang Y. Solid-state proton battery operated at ultralow temperature. *American Chemical Society Energy Letters*. 2020;5:685-691.
11. Valladares L, Salinas D, Dominguez A, Najarro D, Khondaker S, Mitrelias T. Crystallization and electrical resistivity of Cu₂O and CuO obtained by thermal oxidation of Cu thin films on SiO₂/Si substrates. *Thin solid films*. 2012;520:6368-6369.
12. Du BD, Phu DV, Quoc LA, Hien NQ. Synthesis and Investigation of Antimicrobial Activity of Cu₂O Nanoparticles/Zelite. *Journal of Nanoparticles*. 2017;7056864:6.
13. Zhang W, Du L, Chen Z, Hong J, Yue L. ZnO nanocrystals as anode electrodes for lithium-ion batteries. *Journal of Nanomaterials*. 2016;8056302:7. DOI:<http://dx.doi.org/10.1155/2016/8056302>

© 2020 Menegbo et al.; This is an Open Access article distributed under the terms of the Creative Commons Attribution License (<http://creativecommons.org/licenses/by/4.0>), which permits unrestricted use, distribution, and reproduction in any medium, provided the original work is properly cited.

Peer-review history:

The peer review history for this paper can be accessed here:
<http://www.sdiarticle4.com/review-history/58027>